



## MULTI-RESOLUTION ANALYSIS OF TURBULENT CHANNEL FLOWS WITH SPANWISE WALL OSCILLATION

SEJONG CHUN<sup>1c</sup>, EDWARD HURST<sup>2</sup>, YONGMANN M. CHUNG<sup>2</sup>

<sup>1</sup> Division of Physical Metrology, Korea Research Institute of Standards and Science, Daejeon, 305-340, Korea

<sup>2</sup> School of Engineering and Centre for Scientific Computing, University of Warwick, Coventry CV4 7AL, UK

<sup>c</sup>Corresponding author: Tel.: +82-42-868-5311; Fax: +82-42-868-5028; Email: sjchun@kriss.re.kr

### KEYWORDS:

**Main subjects:** turbulent flow, flow visualization

**Fluid:** incompressible flow, low Reynolds number flow

**Visualization method(s):** numerical flow visualization, digital data processing

**Other keywords:** flow control, wavelet analysis, multi-resolution analysis

**ABSTRACT:** Spanwise wall oscillation is a control strategy to suppress streamwise vortices near the wall in a channel flow, leading to significant reduction of skin friction forces in the channel. Since the sweeping and ejection motions of the streamwise vortices enhances mixing between low and high-momentum fluids in the near-wall region, the suppression of streamwise vortices leads to an effective control of the skin friction of the channel. Even though many investigations focused on the effect of skin friction reduction by spanwise wall oscillation, there has not yet been a study regarding a multi-resolution analysis using a discrete wavelet transform. In the present study, the multi-resolution analysis was performed to investigate the scale-resolved streamwise vortices controlled by the spanwise wall oscillation. The maximal overlap discrete wavelet transform (MODWT) was used as a means for the multi-resolution analysis. From this scale-resolved analysis, it was found that the smallest scales rather than larger scales of streamwise vortices were effectively suppressed by the spanwise wall oscillation. It was also conjectured that the Stokes flow, induced by the spanwise wall oscillation, accelerated viscous dissipation of the smallest scale motions, because the spanwise wall oscillation increased frictional motion between the turbulent channel flow and the Stokes flow.

### 1. INTRODUCTION

There are many concerns of reducing skin friction force on the surface of a moving body, because the skin friction force imposes large flow resistance on the moving body, leading to larger energy consumption with higher speeds [1, 2]. There have been a lot of studies to reduce the skin friction force on the moving body in view of flow control. Steady blowing, steady suction, and periodic suction/blowing are typical examples of reducing the skin friction force by providing fluid momentum with the boundary layer flow near the surface of the wall [3, 4]. In case of the periodic suction/blowing, the enhancement of flow structure becomes conspicuous at a certain forcing frequency, because the streamwise vortical structures can be regularized by controlling flow entrainment rates [3, 4]. However, the advantages of the control strategies might not be very effective, when the working fluid does not allow invasive methods for flow control.

A spanwise wall oscillation can give another flow control strategy without inducing additional flows outside from the wall regions. Instead, the spanwise wall oscillation agitates the near-wall turbulent structures by generating Stokes flows [5-8]. At a certain oscillation frequency and amplitude, the streamwise vortical structures can be suppressed as efficiently by the spanwise wall oscillation as reported in the periodic suction/blowing [3-8]. On the while, contrary to the periodic suction/blowing, which is an invasive control method, the spanwise wall oscillation can be a non-invasive control method, because only tangential movement of surrounding surfaces is considered. Therefore, the spanwise wall oscillation can be an ideal flow control strategy in internal flows such as a pipe flow.

One application area for the spanwise wall oscillation would be flow rate measurements in closed conduits [9]. Most flow meters require well-defined flow velocity profiles in a fully-developed turbulent flow for an accurate flow metering. Toward this end, a straight pipe section should be placed upstream of the flow metering station, because



swirling flows, generated by conduit elements such as an elbow and a butterfly valve, can affect flow metering significantly [9]. However, the length of the straight pipe can impose space limitations in a practical situation, because the straight pipe should be more than 30 times of the conduit diameter to reduce the swirling flow effectively. The spanwise wall oscillation might suggest a method to solve such space limitations by suppressing the streamwise vortical structures. The spanwise wall oscillation can dissipate the turbulent kinetic energy induced by the swirling flows, because the streamwise vortical structures can be dissipated effectively by the spanwise wall oscillation [5, 6, 7].

As a first step toward developing such a non-invasive flow control strategy, the effect of spanwise wall oscillation was investigated in a turbulent channel flow by direct numerical simulation (DNS). Maximal overlap discrete wavelet transform (MODWT) was employed as a tool for multi-resolution analysis of the turbulent channel flow [10, 11]. Swirling strength was derived from the scale-resolved velocity field to induce meaningful information from the spatially-resolved flow fields [12, 13]. The purpose of the multi-resolution analysis was to elucidate the effect of the spanwise wall oscillation by scale resolution. Because three-dimensional data at a specified time were provided by the DNS, the MODWT was performed in the streamwise direction. From the scale-resolved analysis, it was found that the streamwise vortical structures near the channel wall was effectively suppressed by the spanwise wall oscillation. On the other hand, the central region in the flow velocity profile became smoother, or relaminarized, by the spanwise wall oscillation [5, 6, 7].

## 2. NUMERICAL ANALYSIS METHODS

### 2.1 Numerical method to simulate a turbulent channel flow

A DNS was performed to simulate the turbulent channel flow at Reynolds number with  $Re_\tau = 200$ , based on the friction velocity and the channel half-height [1, 2, 14].

$$Re_\tau = u_\tau \delta / \nu \quad (1)$$

Here,  $u_\tau$  is the friction velocity,  $\delta$  is the half-height of the channel, and  $\nu$  is the kinematic viscosity. All the dimensions of the channel were denoted in terms of wall units [1, 2, 14]. The dimensions were 9 in the  $x$  direction, 2 in the  $y$  direction, and 4 in the  $z$  direction, as shown in Fig. 1. The number of grids in the numerical domain was defined as 128 ( $x$  direction)  $\times$  129 ( $y$  direction)  $\times$  128 ( $z$  direction). At the top and bottom walls of the channel in the  $y$  direction, i.e., at  $y = 0$  and 2, no-slip condition was imposed to define them as rigid walls. However, periodic boundary conditions were applied to both side walls in the  $z$  direction, i.e., at  $z = 0$  and 4. Inflow and convective boundary conditions along the streamwise direction ( $x$  direction) were applied to the inlet and the outlet located at  $x = 0$  and  $x = 8$ , respectively. Therefore, an initially quiescent flow could be developed into the fully-developed turbulent flow by the numerical simulation. More detailed explanations on the DNS can be found in the previous studies [1, 2].

### 2.2 Maximal overlap discrete wavelet transform

A MODWT is a kind of discrete wavelet transform, which can be used to investigate the spatial distribution of the streamwise velocity distribution along the  $x$ ,  $y$ , or  $z$  directions in the channel flow. The MODWT is suitable for a multi-resolution analysis (MRA) which describes the spatial and the temporal evolution of turbulent flows, because the MODWT can delineate small vortical structures by decomposing the streamwise velocity into detail and smooth components [10].

$$u(y, z) = \sum_{j=1}^n u_{D_j}(y, z) + u_{S_n}(y, z) \quad (2)$$

Here,  $u$  is the streamwise velocity,  $y$  is the wall-normal direction,  $z$  is the spanwise direction,  $n$  is the number of scales for the MRA,  $D_j$  is the  $j$ -th level detail component by the MODWT, and  $S_n$  is the  $n$ -th level smooth component. Note that  $D_j$  looks like a band-pass filter at  $j$ -th level scale, while  $S_n$  plays a role as a low-pass filter to complete the MRA at  $n$ -th level scale [10].

The MODWT can be implemented by a pyramid algorithm, which calculates  $D_j$  and  $S_j$  by circularly convoluting both the wavelet filter  $\tilde{H}$  and the scaling filter  $\tilde{G}$  at each scale, as shown in Fig. 2. Here,  $\tilde{W}_j$  and  $\tilde{V}_j$  are the wavelet and the scaling coefficients to calculate  $D_j$  and  $S_j$ .  $\tilde{0}_j$  is a zero-valued vector.  $2^{j-1}k/N$  is a kind of circular filter, which can



adjust phase shifts by the band-pass or the low-pass filters [10]. Although the MODWT is developed to analyse time-series data, the MODWT can be also applied for spatially distributed flow field at a specified instant. In case of the numerical study, the DNS can provide the spatially distributed flow field with very high precision [1-8]. In this case, an appropriate selection for analysis direction ( $x$ ,  $y$ , or  $z$ ) becomes necessary, because the spatial resolution of each direction will determine the resolved scales by the multi-resolution analysis. It is noticed that the spatial resolution in the  $x$  direction is located between 0.14 and 4.5 wall units. However, in the  $y$ , or the  $z$  directions, the spatial resolution becomes reduced down to (0.03 ~ 1) and (0.06 ~ 2) wall units, respectively. This means that the spatial resolutions in these directions are too small to analyze the flow field.

### 2.3 Spanwise wall oscillation

A spanwise wall oscillation was implemented by applying a sinusoidal function with a certain amplitude and frequency to the top and the bottom walls ( $y = 0$  and  $2$ ).

$$w_1 = W_1 \sin(\omega t) \quad (3)$$

Here,  $w_1$  is the spanwise displacement in the wall units,  $W_1$  is the amplitude of wall oscillation,  $\omega$  is the frequency of wall oscillation, and  $t$  is time.  $W_1$  was defined as 27 in the wall units, and the oscillation period  $2\pi/\omega$  was set to be 100 in the wall units [1, 2, 8]. The effect of spanwise wall oscillation could be found by comparing the streamwise and the spanwise velocity profiles as shown in Figs. 4 and 5. Near the top and the bottom walls, the spanwise velocity components were prominent in case of the spanwise wall oscillation. As a result of this, velocity defects were observed at the same region of the streamwise velocity profiles by the spanwise wall oscillation.

### 2.4 Swirling strength

Swirling strength is a useful mathematical tool to identify vortices buried in turbulent flows [12, 13]. The swirling strength can be calculated with the characteristic equation of a velocity gradient tensor. Even though a three-dimensional tensor can be also used for obtaining the swirling strength, two-dimensional one is better for understanding and implementing a suitable algorithm [12, 13]. In calculating the swirling strength, an imaginary part of a complex conjugate eigenvalue is sought. The two-dimensional velocity gradient tensor is denoted as follows.

$$d^{2D} = \begin{bmatrix} \frac{\partial v}{\partial y} & \frac{\partial v}{\partial z} \\ \frac{\partial w}{\partial y} & \frac{\partial w}{\partial z} \end{bmatrix} \quad (4)$$

Here,  $d^{2D}$  means the two-dimensional velocity gradient tensor. Actually,  $d^{2D}$  is the Jacobian matrix of a two-dimensional vector  $(v(y, z), w(y, z))$ . The characteristic equation of  $d^{2D}$  can be written as in the following equation.

$$\|d^{2D} - \lambda I\| = \left(\frac{\partial v}{\partial y} - \lambda\right) \left(\frac{\partial w}{\partial z} - \lambda\right) - \frac{\partial v}{\partial z} \frac{\partial w}{\partial y} = 0 \quad (5)$$

Here,  $\lambda$  is an eigenvalue of  $d^{2D}$ ,  $I$  is the identity matrix, and  $\|\cdot\|$  is the determinant symbol of a matrix. In this case, the imaginary parts of solutions to the characteristic equation of  $d^{2D}$  represent the swirling strength in the streamwise direction [12, 13].

## 3. NUMERICAL RESULTS AND DISCUSSIONS

### 3.1 Velocity fields with or without the spanwise wall oscillation

Some numerical results in the cross section of the channel at  $x = 4.5$  are shown in Figs. 6 and 7. In the turbulent channel flow without spanwise wall oscillation, the streamwise velocity distribution is highly turbulent. In the top and the bottom regions of Fig. 6a, irregular velocity distribution is observed, by entrainment of low-momentum fluid at  $y = 0 \sim 0.2$  or  $1.8 \sim 2$  into the upper flow region at  $y = 0.2 \sim 0.5$  or  $1.5 \sim 1.8$ . In the central region ( $y = 0.5 \sim 1.5$ ), momentum transfer between low- and high-momentum fluids is observed at  $(y, z) = (0.8, 1)$ ,  $(1, 3)$ , and  $(1.2, 3.5)$ . The vector plots depicting  $(v, w)$  at  $x = 4.5$  show that the locations of momentum transfer coincide with the swirling motions by secondary flows (Fig. 6b). It is seen that the secondary flow motions are restricted within  $y \leq 0.5$  and  $y \geq$



1.5. In case of the flows with the spanwise wall oscillation, the streamwise velocity distribution becomes regularized smoothly, or relaminarized, compared with the distribution without the spanwise wall oscillation (Fig. 7a) [5-8]. The boundary layer seems to be attached to the wall region ( $y = 0 \sim 0.4, 1.6 \sim 2$ ) more than the boundary layer without the spanwise wall oscillation. Momentum transfer in the central region ( $y = 0.5 \sim 1.5$ ) seems to be weakened, and the velocity distribution becomes more uniform. In the vector plots at  $x = 4.5$  (Fig. 7b), vortical motions are weakened significantly by the spanwise wall oscillation. At the same time, strong spanwise velocity,  $w$  is observed at  $y = 0 \sim 0.2$  and  $1.8 \sim 2$  in the spanwise directions ( $z$ ). It is thought to be the effects of Stokes flows driven by the spanwise wall oscillation [5-8, 15].

### 3.2 Multi-resolution analysis on the velocity fields affected by the spanwise wall oscillation

Although the effect of the spanwise wall oscillation is conspicuous by investigating the velocity fields at the cross section of the channel, the analysis would not be sufficient to describe the effect of the spanwise wall oscillation without considering a scale-resolved analysis. Looking at the streamwise velocity distribution in Fig. 6, the flow patterns seem to have more spiky structures than the streamwise flow patterns shown in Fig. 7. This might mean that the vortical structures with smaller spatial scales are abundant in the turbulent channel flow without the spanwise wall oscillation. On the contrary, the small scale vortical structures might be removed in the flow with the spanwise wall oscillation. To find out this assumption, a multi-resolution analysis with suitable streamwise spatial resolution (in the  $x$  direction) was performed and displayed as shown in Figs. 8 and 9. The streamwise velocity distribution of the cross section at  $x = 4.5$  was analysed up to the sixth levels ( $D_1 \sim D_6, S_6$ ). However, in the figures, only three levels are selected to summarize the analytical results ( $D_2, D_4$ , and  $S_6$ ). When the scale-resolved streamwise velocity without the spanwise wall oscillation is scaled with  $u = (-0.04 \sim 0.04)$  at  $D_2$ , it is noticed that most of the velocity components are populated in the near-wall region ( $y = 0 \sim 0.5, 1.5 \sim 2$ ), as seen in Fig. 8a. When the spanwise wall oscillation is applied to the channel flow, the scale-resolved streamwise velocity in the near-wall region is almost disappeared in Fig. 9a.

Similar tendency can also be found with the scale-resolved streamwise velocity at  $D_4$ , as shown in Figs. 8b and 9b. In these plots, the streamwise velocity is scaled with  $u = (-0.12 \sim 0.12)$ . When the channel flow is not disturbed by the spanwise wall oscillation, the scale-resolved streamwise velocity is non-uniformly distributed along the wall regions. On the other hand, the scale-resolved streamwise velocity seems to be regularized at  $(y, z) = (1.8, 1.3 \sim 2.7)$  by the spanwise wall oscillation. The maximum value of the streamwise velocity distribution is reduced by the spanwise wall oscillation (Fig. 9b). In the smooth plots at  $S_6$  (Figs. 8c and 9c), the irregularity, which can be found in the wall region of the channel flow without the spanwise wall oscillation, turns to uniformity in the same region of the channel flow with the spanwise wall oscillation. Additionally, the boundary layer, located in  $0 \leq y \leq 0.1$  and  $1.9 \leq y \leq 2$ , becomes thickened at this spatial resolution ( $S_6$ ) by the spanwise wall oscillation. Therefore, it can be said that the spanwise wall oscillation suppresses the streamwise velocity distribution effectively at the smaller spatial scale ( $D_2$ ). After that, the velocity distribution becomes regularized at the subsequent spatial scales ( $D_4$ ). Finally, the velocity distribution at the largest spatial scale ( $S_6$ ) becomes uniform at the wall region.

The effect of the spanwise wall oscillation can be ascertained when the velocity vectors are drawn, as suggested in Figs. 10 and 11. Because the velocity vectors portray vortical motions of secondary flows at the cross section of  $x = 4.5$ , most of the vortical motions are found to be located in the wall regions ( $y = 0 \sim 0.5, 1.5 \sim 2$ ). If the same unit velocity of 0.2 is maintained throughout the other velocity plots, the strongest vortical motions are observed at  $D_4$  when the spanwise wall oscillation is not applied to the channel flow, as seen in Fig. 10b. Other scales ( $D_2$  and  $S_6$ ) have relatively weak vortical motions (Figs. 10a, 10c). When the spanwise wall oscillation is applied to the channel flow, most of the vortical motions are disappeared at  $D_4$  (Fig. 11b), and the vortical motions at the other scale ( $D_2$ ) are also reduced noticeably (Fig. 11a). At  $S_6$ , the velocity vectors in the near-wall regions ( $y = 0 \sim 0.1, 1.9 \sim 2$ ) are vaguely described, because there are regions with strong spanwise velocity component in the  $z$  direction (Fig. 11c).

### 3.3 Swirling strength of the scale-resolved velocity fields affected by the spanwise wall oscillation

Swirling strength, based on the velocity plots at the cross section of the channel flow, is calculated to correlate locations of vortical motions with the streamwise vorticity, as seen in Figs. 12 and 13. Most of the swirling strength reside in the wall regions ( $y = 0 \sim 0.5, 1.5 \sim 2$ ). The locations with strong swirling strength, drawn in red colour, are coincident with the center of the vortical motions drawn in the vector plots (Figs. 10 and 11). This means that the



vortical motions, which have strong swirling strength, can be regarded as streamwise vortices. However, the locations with the strong swirling strength are not exactly the same as the locations where strong streamwise velocity was distributed. This might be related with sweeping events of the streamwise vortices, which occurs intermittently by mixing between the low and the high momentum fluids [3-8].

At each spatial scale, i.e.,  $D_2$  and  $D_4$ , the swirling strength is reduced by the spanwise wall oscillation. In Figs. 12a and 13a, remarkable reduction of the swirling strength at  $D_2$  is observed. It is because the small scale motions of the streamwise vortices are suppressed by the spanwise wall oscillation. The suppression of the small vortical structures is caused by the Stokes flow in the spanwise direction at the near-wall regions ( $y = 0 \sim 0.1$  and  $1.9 \sim 2$ ) [1, 5-8]. When the Stokes flow is superimposed on the boundary layer flow near the wall, the flow generates large velocity gradients to the streamwise vortices. This resembles a milling process of a machining tool on the irregular surface of a work piece. This means that the smallest spatial motions of the streamwise velocity are wiped out by heat dissipation due to the large velocity gradients generated by the Stokes flow near the wall. This might be the reason for reduction of the small spatial scales of the streamwise vortices by the spanwise wall oscillation.

In addition, when the oscillation frequency is in order of the intermittent frequency of the sweeping or ejection events of the streamwise vortices, the mixing between the low and the high momentum fluids are effectively prevented [5-8]. Therefore, it can be conjectured that the superimposed Stokes flow not only accelerates the energy transfer from the largest to the smallest spatial scales via increased heat dissipation of the smallest scale streamwise velocity, but also hinders turbulent mixing from the smallest to the larger spatial scales of flow motions. Therefore, the channel flow loses most of its energy by the spanwise wall oscillation, and the flow becomes laminar again (relaminarization) [5-8].

This feature of the spanwise wall oscillation as a role of suppressing the turbulent flow structures can be visualized in a three-dimensional reconstruction of swirling strengths as shown in Figs. 14 and 15. These figures are iso-contour plots of swirling strengths with a certain iso-contour levels ( $s = 1$  for the DNS data,  $s = 0.3$  and  $0.4$  for the scale-resolved data). The three-dimensional reconstruction was performed by combining the swirling strength distribution at the cross section from  $x = 0$  to  $x = 9$  along the streamwise direction ( $x$ ). The reconstructed streamwise vortices show both the sweeping and the ejection events, and these streamwise structures enable mixing between the low momentum fluid at the wall region ( $y = 0 \sim 0.5$  or  $1.5 \sim 2$ ) and the high momentum fluid at the central region ( $y = 0.5 \sim 1.5$ ) [3-8].

The role of the streamwise vortices for sustaining turbulence levels in the channel flow is reduced by the spanwise wall oscillation. In the flow without the spanwise wall oscillation, the streamwise vortices are irregularly distributed, such that the distribution affects the non-uniform distribution of streamwise velocity as indicated by Figs. 6a and 14a. However, in the flow with the spanwise wall oscillation, the number of streamwise vortices with the same swirling strength ( $s = 1$ ) was significantly reduced in Fig. 15a. The distribution of the streamwise vortices seems to be more uniform than the case without the spanwise wall oscillation. Therefore, the streamwise velocity distribution at the cross section of  $x = 4.5$  becomes more uniform in the central region, because the turbulent mixing between the low and the high momentum fluids is weakened by the spanwise wall oscillation.

If the spatially resolved swirling strength distributions at  $D_2$  and  $D_3$  are combined along the streamwise direction, it can be visualized that the streamwise vortices are effectively suppressed by the spanwise wall oscillation (Figs. 14b and 15b, 14c and 15c). However, at the spatial scales larger than  $D_3$ , the suppression of the streamwise vortices by the spanwise wall oscillation is not conspicuous as in the smaller spatial scales ( $D_2$  and  $D_3$ ). This means that the spanwise wall oscillation was responsible for inhibiting the turbulent mixing between the low and the high momentum fluids by suppressing the small spatial scales of streamwise vortical structures. It is also noticeable that the ejection modes of the streamwise vortices were found at  $D_2 \sim D_3$ . This means that the suppression of the small spatial scales of streamwise vortices has a crucial role to the hindrance of the turbulent mixing between the low and the high momentum fluids.

#### 4. CONCLUSIONS

Spanwise wall oscillation is one of good flow control strategies for suppressing streamwise vortical structures near the wall in a channel flow, leading to significant reduction of skin friction forces in the channel. Even though many investigations focused on the effect of spanwise wall oscillation on the turbulent flow control, there has not been a study regarding spatial scale-resolved analysis on the streamwise vortical structured underlying the turbulent channel flows with the spanwise wall oscillation. As an efficient method of spatial scale resolution, a maximal overlap discrete wavelet transform (MODWT) was employed. The definition of swirling strength was introduced to find the location of streamwise vortical structures from the velocity plots at the cross section of the channel flow.



The major finding of the present study was that the smallest spatial scale motions of the streamwise velocity and the streamwise vortices were effectively suppressed by the spanwise wall oscillation. It was because the Stokes flow due to the spanwise wall oscillation superimposed large velocity gradients to the small scale flow motions at the near-wall regions. This might cause significant reduction of streamwise vortical strength at the smallest scales by heat dissipation. On the contrary, the large scale flow motions at the central region became uniform by the spanwise wall oscillation. This was due to the hindrance of the turbulent mixing between the low and the high momentum fluids, which was conducted by sweeping and ejection motions of the streamwise vortices near the wall region. The reduction of the turbulent mixing caused the relaminarization of the turbulent channel flow by the spanwise wall oscillation.

## References

1. Chung Y. M. and Talha T. *Effectiveness of active flow control for turbulent skin friction drag reduction*. Phys. Fluids 2011, **23** (2), 025102 (pp. 1070-6631)
2. Elam D. T. and Chung Y. M. *Numerical simulation of plasma actuators for turbulent skin friction drag reduction*. Proc. of EDRFCM-2010, Kiev, Ukraine, 2-4 September, 2010
3. Choi H., Moin P. and Kim J. *Active turbulence control for drag reduction in wall-bounded flows*. J. Fluid Mech. 1994, **262**, pp.75-110
4. Lee C., Kim J., Babcock D. and Goodman R. *Application of neural networks to turbulence control for drag reduction*. Phys. Fluids, 1997, **9**, pp. 1740-1747
5. Baron A. and Quadrio M. *Turbulent drag reduction by spanwise wall oscillation*. Appl. Sci. Research, 1996, **55**, pp. 311-326
6. Quadrio M. and Ricco P. *Critical assessment of turbulent drag reduction through spanwise wall oscillations*. J. Fluid Mech. 2004, **521**, pp.251-271
7. Quadrio M. and Ricco P. *The laminar generalized Stokes layer and turbulent drag reduction*. J. Fluid Mech. 2011, **667**, pp. 135-157
8. Choi J. I., Xu C. X. and Sung H. J. *Drag reduction by spanwise wall oscillation in wall-bounded turbulent flows*. AIAA J. 2002, **40**(5), pp. 842-850
9. *ISO Measurement of fluid flow by means of pressure differential devices inserted in circular cross-section conduits running full*. ISO5167:1-4, International Organization for Standardization, Geneva, Swiss, 2003
10. Percival D. B. and Walden A. T. *Wavelet methods for time series analysis*. Cambridge University Press, New York, USA, 2000
11. Chun S., Liu Y. Z. and Sung H. J. *Multi-resolution analysis of the large-scale coherent structure in a turbulent separation bubble affected by an unsteady wake*. J. Fluids and Struct. 2007, **23**, pp. 85-100
12. Adrian R. J., Christensen K. T. and Liu Z. -C. *Analysis and interpretation of instantaneous turbulent velocity fields*. Exp. Fluids 2000, **29**, pp. 275-290
13. Bryant D. B., Seol D. -G. and Socolofsky S. A. *Quantification of turbulence properties in bubble plumes using vortex identification methods*. Phys. Fluids 2009, **21**, 075101 (pp. 1-10)
14. Pope S. B. *Turbulent flow*. Cambridge University Press, Cambridge, UK, 2000
15. Currie I. G. *Fundamental mechanics of fluids*. CRC Press, New York, USA, 2002

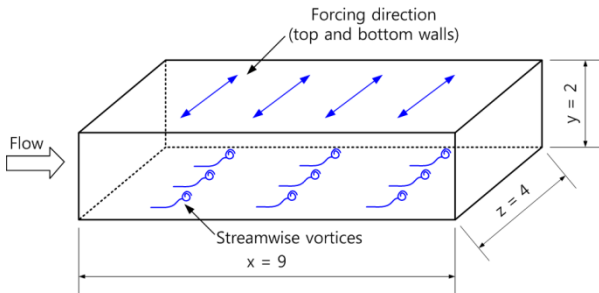
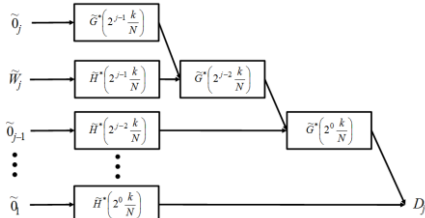


Fig. 1 Schematic of the system for a turbulent channel flow with spanwise wall oscillation,  $x$ ,  $y$  and  $z$  are the dimensions of the computational domain

(a)  $j$ -th level detail,  $D_j$



(b)  $j$ -th level smooth,  $S_j$

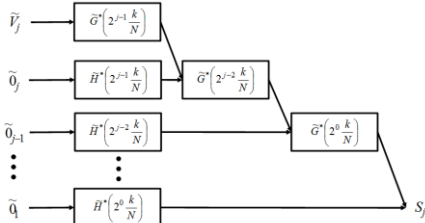
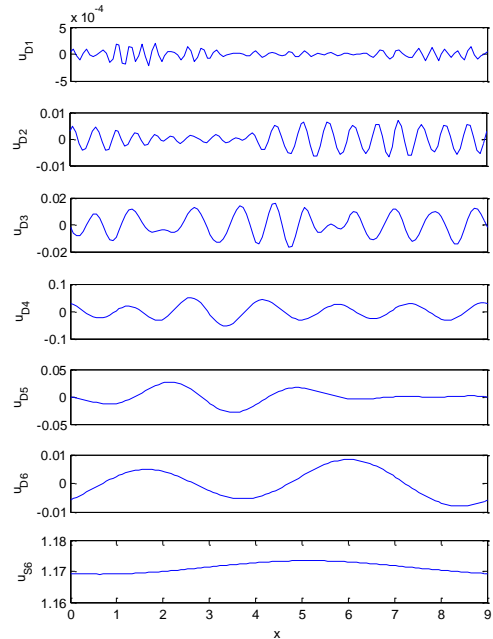


Fig. 2 Flow chart for calculating the MODWT in terms of  $D_j$  and  $S_j$

(a) Multi-resolution analysis



(b) Validation of analysis

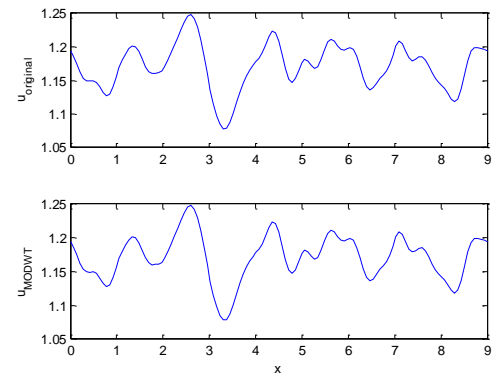


Fig. 3 Multi-resolution analysis of a streamwise velocity signal along the  $x$  direction at  $(y, z) = (1, 2)$

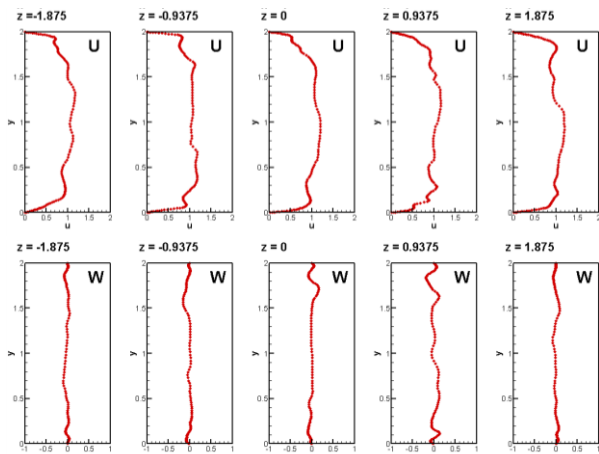


Fig. 4 Velocity profiles of streamwise and spanwise velocity components at  $x = 4.5$  without spanwise wall oscillation

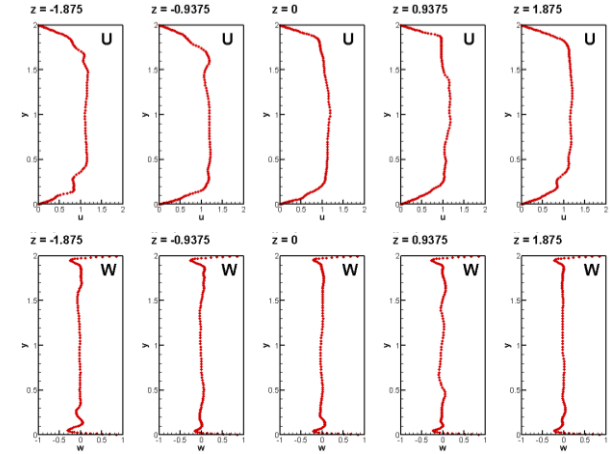


Fig. 5 Velocity profiles of streamwise and spanwise velocity components at  $x = 4.5$  with spanwise wall oscillation

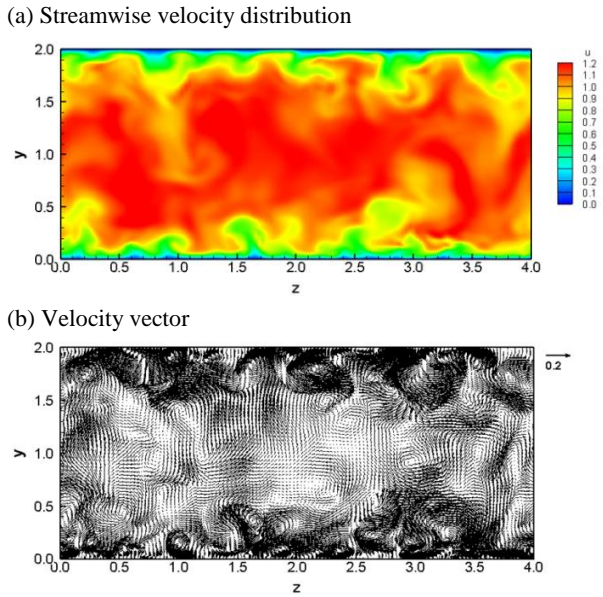


Fig. 6 Velocity plots of the cross section in a channel flow at  $x = 4.5$  without spanwise wall oscillation

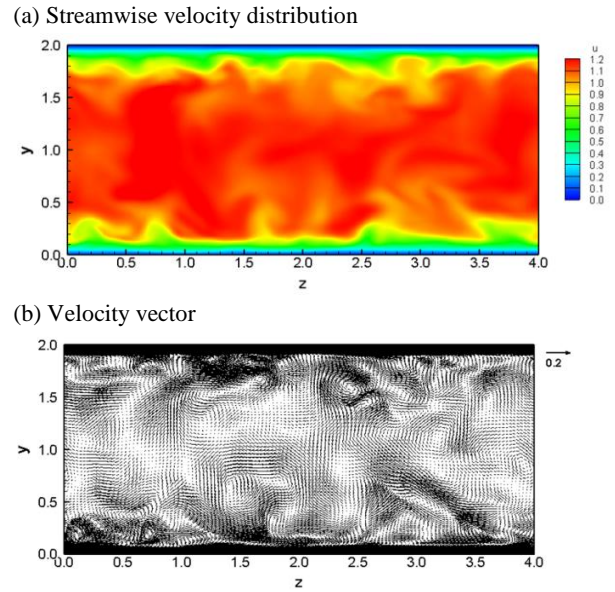


Fig. 7 Velocity plots of the cross section in a channel flow at  $x = 4.5$  with spanwise wall oscillation

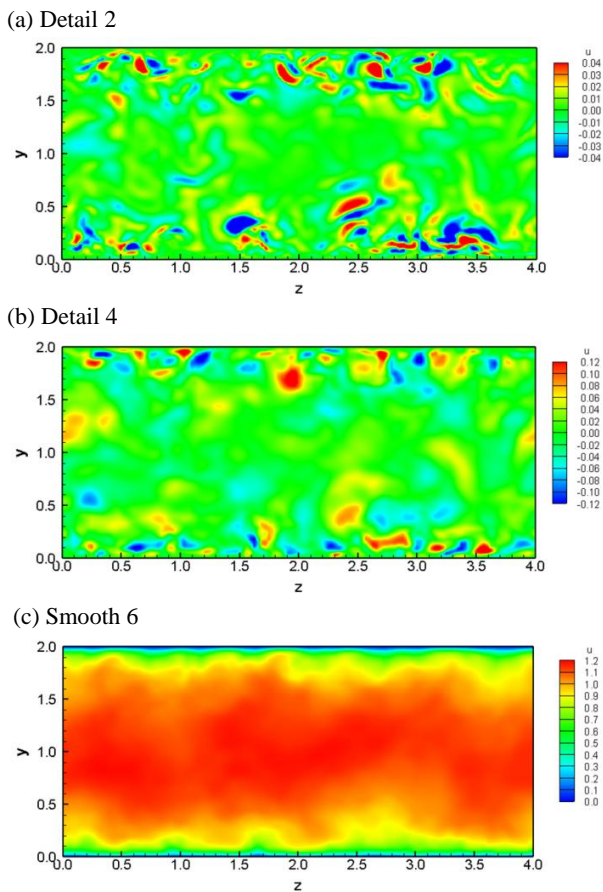


Fig. 8 Velocity plots of the cross section in a channel flow at  $x = 4.5$  without spanwise wall oscillation

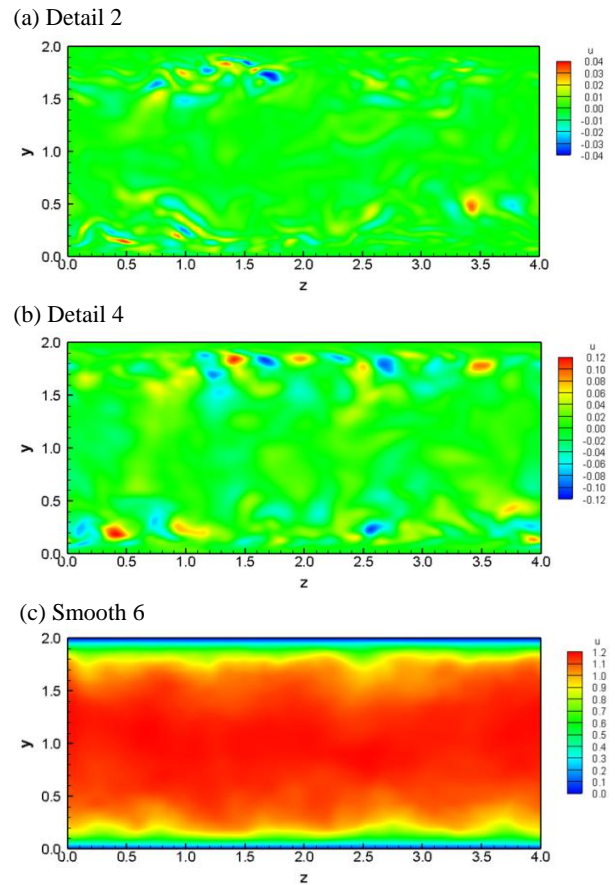


Fig. 9 Velocity plots of the cross section in a channel flow at  $x = 4.5$  with spanwise wall oscillation

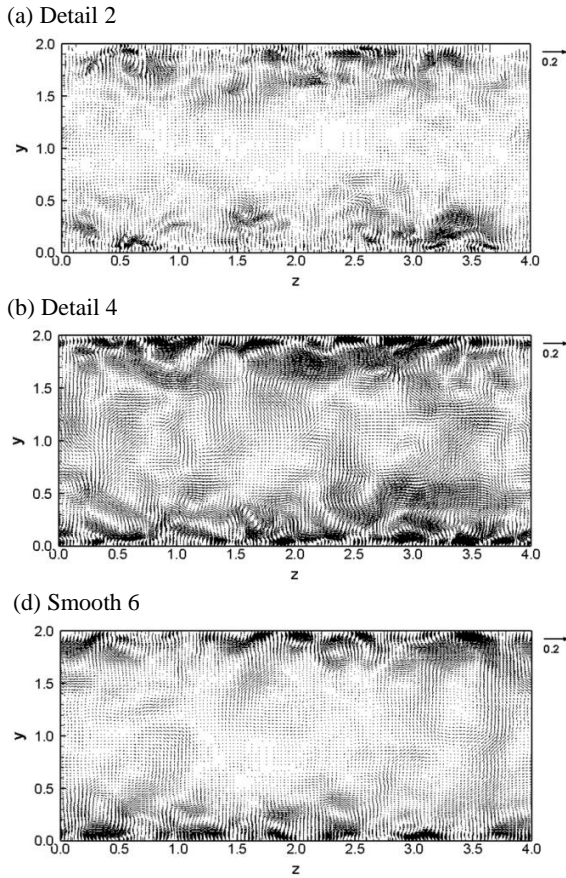


Fig. 10 Velocity plots of the cross section in a channel flow at  $x = 4.5$  without spanwise wall oscillation

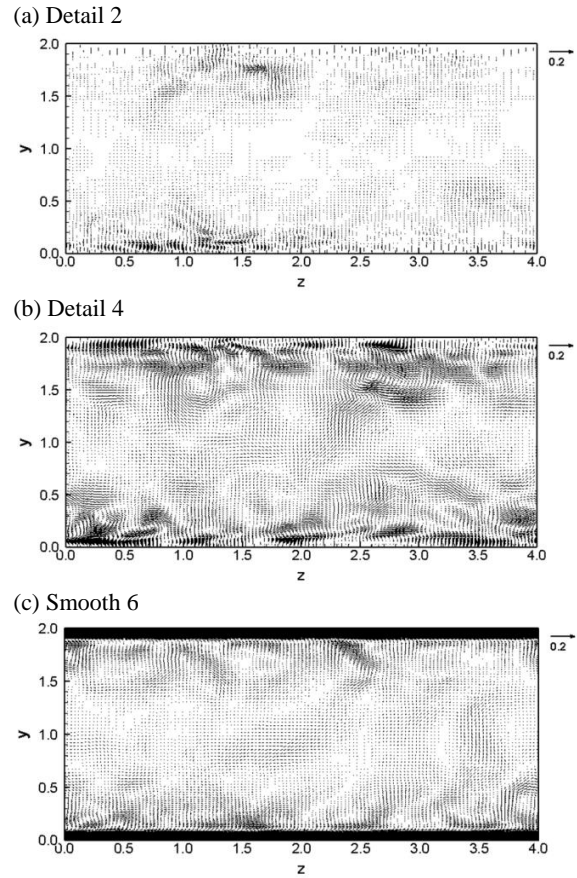


Fig. 11 Velocity plots of the cross section in a channel flow at  $x = 4.5$  with spanwise wall oscillation

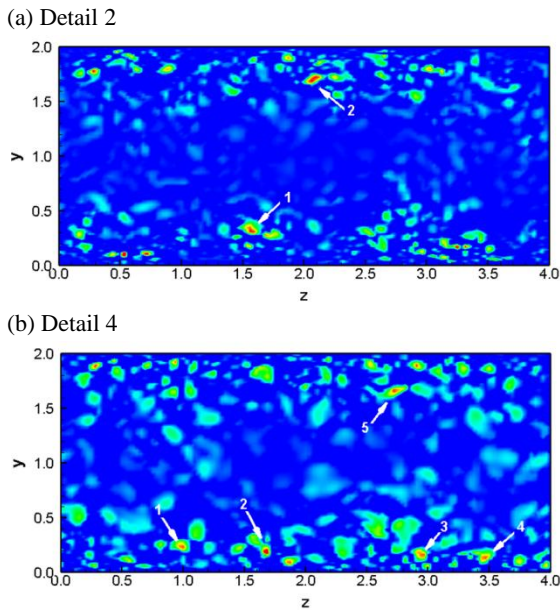


Fig. 12 Swirling strength in the streamwise direction at  $x = 4.5$  without spanwise wall oscillation

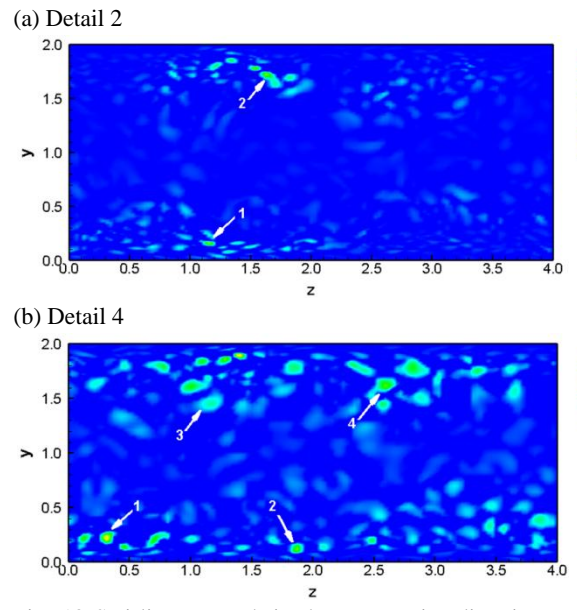
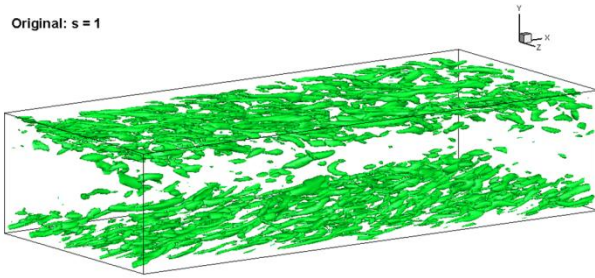


Fig. 13 Swirling strength in the streamwise direction at  $x = 4.5$  with spanwise wall oscillation



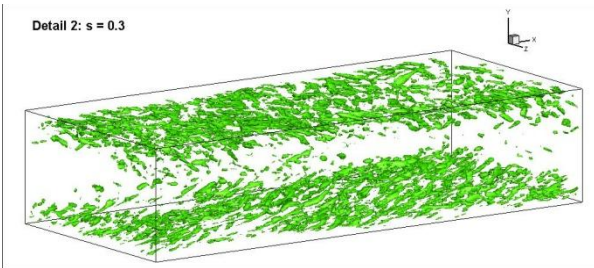
(a) Original data

Original:  $s = 1$



(b) Detail 2

Detail 2:  $s = 0.3$



(c) Detail 3

Detail 3:  $s = 0.4$

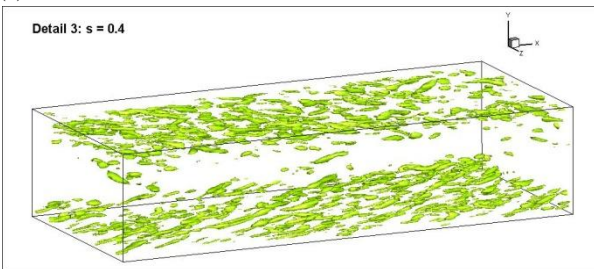
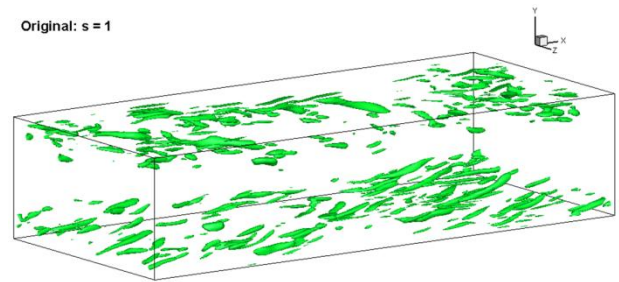


Fig. 14 Iso-contour of streamwise vorticity in terms of swirling strength at  $x = 4.5$  without spanwise wall oscillation

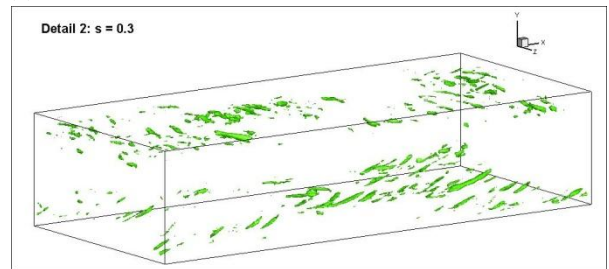
(a) Original data

Original:  $s = 1$



(b) Detail 2

Detail 2:  $s = 0.3$



(c) Detail 3

Detail 3:  $s = 0.4$

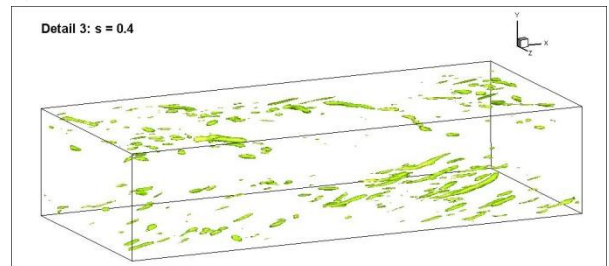


Fig. 15 Iso-contour of streamwise vorticity in terms of swirling strength at  $x = 4.5$  with spanwise wall oscillation